

Thermal and mechanical properties and micro-mechanism of SiO_2/epoxy nanodielectrics

Tian-Yu Wang(王天宇), Gui-Xin Zhang(张贵新), and Da-Yu Li(李大雨)
Citation: Chin. Phys. B, 2021, 30 (**12**): 128101. DOI: 10.1088/1674-1056/abff2c
Journal homepage: http://cpb.iphy.ac.cn; http://iopscience.iop.org/cpb

What follows is a list of articles you may be interested in

Prediction of structured void-containing 1T-$PtTe_2$ monolayer with potential catalytic activity for hydrogen evolution reaction

Bao Lei(雷宝), Yu-Yang Zhang(张余洋), Shi-Xuan Du(杜世萱)
Chin. Phys. B, 2020, 29 (**5**): 058104. DOI: 10.1088/1674-1056/ab8203

Density functional calculations of efficient H_2 separation from impurity gases (H_2, N_2, H_2O, CO, Cl_2, and CH_4) via bilayer g-C_3N_4 membrane

Yuan Guo(郭源), Chunmei Tang(唐春梅), Xinbo Wang(王鑫波), Cheng Wang(王成), Ling Fu(付玲)
Chin. Phys. B, 2019, 28 (**4**): 048102. DOI: 10.1088/1674-1056/28/4/048102

Thermal conduction of one-dimensional carbon nanomaterials and nanoarchitectures

Haifei Zhan(占海飞), Yuantong Gu(顾元通)
Chin. Phys. B, 2018, 27 (**3**): 038103. DOI: 10.1088/1674-1056/27/3/038103

Molecular dynamics study of anisotropic growth of silicon

Naigen Zhou(周耐根), Bo Liu(刘博), Chi Zhang(张弛), Ke Li(李克), Lang Zhou(周浪)
Chin. Phys. B, 2016, 25 (**7**): 078109. DOI: 10.1088/1674-1056/25/7/078109

Molecular dynamics simulation on generalized stacking fault energies of FCC metals under preloading stress

Zhang Liang, Lü Cheng, Tieu Kiet, Zhao Xing, Pei Lin-Qing, Michal Guillaume
Chin. Phys. B, 2015, 24 (**8**): 088106. DOI: 10.1088/1674-1056/24/8/088106

Thermal and mechanical properties and micro-mechanism of SiO_2/epoxy nanodielectrics*

Tian-Yu Wang(王天宇), Gui-Xin Zhang(张贵新)†, and Da-Yu Li(李大雨)

Department of Electrical Engineering, Tsinghua University, Beijing 100084, *China*

(Received 9 March 2021; revised manuscript received 7 April 2021; accepted manuscript online 8 May 2021)

In addition to electrical insulation properties, the thermal properties of nanodielectrics, such as glass transition temperature, thermal expansion coefficients, thermal conductivity, and mechanical properties, including Young's modulus, bulk modulus, and shear modulus, are also very important. This paper describes the molecular dynamics simulations of epoxy resin doped with SiO_2 nanoparticles and with SiO_2 nanoparticles that have been surface grafted with hexamethyldisilazane (HMDS) at 10% and 20% grafting rates. The results show that surface grafting can improve certain thermal and mechanical properties of the system. Our analysis indicates that the improved thermal performance occurs because the formation of thermal chains becomes easier after the surface grafting treatment. The improved mechanical properties originate from two causes. First, doping with SiO_2 nanoparticles inhibits the degree of movement of molecular chains in the system. Second, the surface grafting treatment weakens the molecular repulsion between SiO_2 and epoxy resin, and the van der Waals excluded region becomes thinner. Thus, the compatibility between SiO_2 nanoparticles and polymers is improved by the grafting treatment. The analysis method and conclusions in this paper provide guidance and reference for the future studies of the thermal and mechanical properties of nanodielectrics.

Keywords: nanodielectric, surface grafting treatment, molecular dynamics simulation, interface properties

PACS: 81.07.Nb, 82.35.Lr, 82.35.Np, 82.20.Wt **DOI:** 10.1088/1674-1056/abff2c

1. Introduction

Epoxy resin (EP) is widely used in the field of insulation due to its excellent insulating properties, chemical stability, good mechanical properties, and low cost. However, with the increasing demand for electricity and the trend towards the miniaturization and integration of electrical equipment, ever-greater requirements for the various aspects of EP performance are being raised. Doping the insulating material with nanoparticles can effectively improve the insulating properties, thermal properties, and mechanical properties.[1–5] However, there are a large number of hydroxyl groups and unsaturated bonds on the surface of common nanoparticles (such as SiO_2), and so the nanoparticles are in a highly chemically active and unstable state. Thus, they can easily agglomerate with other nanoparticles during the preparation of nanodielectrics, resulting in poor affinity with the polymer matrix (such as EP).[6] Some researchers have grafted a silane coupling agent to the nanoparticle surface to reduce the number of surface hydroxyl groups, and found that inhibiting the accumulation of surface charge and increasing the volume resistivity is more effective than pure SiO_2 nanoparticle doping.[6,7] Therefore, applying this surface grafting treatment to nanoparticles to reduce the surface hydroxyl content and then doping EP is a promising means of improving performance. However, to date, there have been few studies of the thermal and mechanical properties of doped surface-grafted nanoparticles in polymers. These properties of nanodielectrics are also very important for practical applications. Additionally, more importantly, owing to the limitations of the current experimental conditions, the change in the micro-mechanism of nanodielectrics after the grafting treatment remains unclear. Therefore, in this article, we will try to solve the above problems.

With the rapid development of computer science, molecular dynamics (MD) simulation technology is being widely used for new material design and polymer synthesis.[8–10] At the same time, the MD simulations can analyze materials on an atomic scale, allowing the macro performance and micro structure of the material to be combined. In recent years, some scholars have studied the properties of EPs and their composite materials through MD simulations,[11–15] and the results obtained by MD simulation are basically the same as the actual experimental results,[11–21] indicating that the results of MD simulation have high reliability. At present, MD simulation has gradually become one of the important scientific research methods.[22] For example, Wang *et al.*[23] and Shen *et al.*[24] conducted the MD simulations of epoxy resin doped with C_{60} and graphene, and they found that the relative permittivity of the system was reduced. Shen *et al.* performed MD simulations on graphene/epoxy resin composites and studied the influence of the number of layers and the size of the graphene on the thermal conductivity of the polymer.[11] Wang *et al.* analyzed the covalent bonds of the SiO_2/epoxy nanocomposite interface through the molecular simulations and believed that the

*Project supported by the National Key Research and Development Program of China (Grant. Nos. 2017YFB0902503 and 2016YFB0900802).

†Corresponding author. E-mail: guixin@mail.tsinghua.edu.cn

© 2021 Chinese Physical Society and IOP Publishing Ltd

covalent bonds formed at the interface are the reason for the increase in the glass transition temperature of the polymer and the reduction in the mobility of the molecular segments.[12] Fasanelia and Sundararaghavan simulated the thermal conductivity of single-walled carbon nanotube/epoxy resin composites and studied the changes in thermal conductivity of composites doped with different types of single-walled carbon nanotube.[13] Gou *et al.* studied the interactions at the interface between single-walled carbon nanotubes and epoxy resin.[14] Jung *et al.* simulated the doping of nitrogen-modified carbon nanotubes into epoxy resin and found that the mechanical properties of the polymers were improved.[15]

In our previous work, we found experimentally that the epoxy resin doped with SiO_2 nanoparticles grafted with hexamethyldisilazane (HMDS) on the surface can effectively inhibit the surface charge accumulation, increase the volume resistivity, and improve the insulation performance.[6] Thus, in this study, the MD simulations are used to investigate the doping of EP with traditional SiO_2 nanoparticles and with SiO_2 nanoparticles grafted with hexamethyldisilazane (HMDS) at surface grafting rates of 10% and 20%, respectively. The thermal and mechanical properties of these nanodielectrics and the microscopic mechanisms are studied in depth, and the conclusions obtained will provide guidance for the analysis and design of nanodielectrics in the future.

2. Methods

2.1. Model construction

2.1.1. Model structure and MD simulation

All MD simulations described in this work were conducted using Materials Studio 8.0. The EP molecule constructed in this study was bisphenol-A epoxy resin (DGEBA). The curing agent was an amine curing agent (593 curing agent, the adducts of diethylene triamine and butyl glycidyl ether). Diagrams of the molecular structures are shown in Fig. 1(a). The DGEBA molecule (degree of polymerization is 1) has epoxy groups on both ends, and the curing agent molecule has primary and secondary amine groups at one end. Spherical SiO_2 nanoparticles with a radius of 1 nm were constructed. Owing to a large number of unsaturated bonds on the surface of the constructed SiO_2, hydroxyl groups were added to the surface to ensure consistency with the actual situation. The SiO_2 nanoparticles are shown in Fig. 1(b). The reason why SiO_2 nanoparticles with a smaller particle size are selected for the simulation in this paper is that if the size of the nanoparticles is normal (such as tens of nanometers), then the entire system will be very large. Limited by the computing power of the computer, each simulation experiment lasted a very long time. Since this work is devoted mainly to the study of physical properties and microstructure, if the entire system is scaled up or down, these properties will not be changed. These SiO_2 nanoparticles were then surface grafted with HMDS. The reaction equation for the surface grafting treatment is shown in Fig. 2(a). The SiO_2 nanoparticles with surface grafting rates of 10% and 20% were constructed (that is, 10% and 20% of the hydroxyl groups on the surface were replaced by HMDS). The surface-modified SiO_2 nanoparticles are shown in Fig. 1(c).

A three-dimensional amorphous unit cell of each model was then constructed. Four models were constructed in this study, namely pure EP, EP doped with SiO_2 nanoparticles (SiO_2/EP), SiO_2 nanoparticles with a surface grafting rate of 10% (10%-SiO_2/EP), and SiO_2 nanoparticles with a surface grafting rate of 20% (20%-SiO_2/EP). Table 1 shows the nanoparticle number and mass percentage of each molecule.

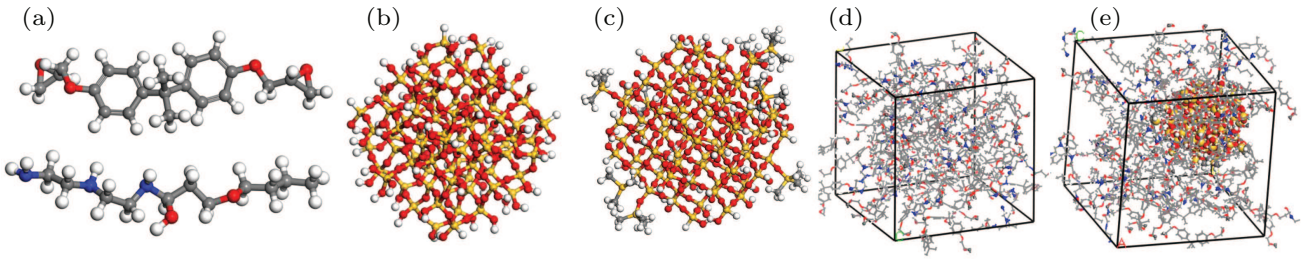


Fig. 1. Schematic diagram of molecular structure of model, showing (a) epoxy resin molecules (top) and curing agent molecules (bottom), (b) SiO_2 nanoparticles with a radius of 1 nm, (c) SiO_2 nanoparticles after surface grafting with HMDS (surface grafting rate 20%), (d) EP and (e) nanocomposite doped with SiO_2 nanoparticles (this panel shows 20%-SiO_2/EP), with white, gray, red, blue, and yellow balls representing H, C, O, N, and Si atoms, respectively.

Table 1. Amorphous unit cell composition of composite system.

Type	Quantity	Percent molecular weight
SiO_2, 10%-SiO_2, 20%-SiO_2	1, 1, 1	16.39, 17.12, 17.84
DGEBA molecule	60	62.26, 61.72, 61.19
Curing-agent molecule	30	21.34, 21.16, 20.97

The initial density was set to be 0.6 g/cm^3. With the subsequent structural optimization and other steps, the density of the system gradually approached to the actual density. All simulations described in this paper used the COMPASS force field. Atom-based method and the Eward method were used to calculate the van der Waals interaction and the electrostatic interaction, respectively, and the simulation quality was set to be medium.

2.1.2. Optmization of model structure

The structure of the three-dimensional amorphous unit cell was optimized to find the structure with the lowest energy. First, the steepest descent algorithm was used to optimize 3000 steps, and then the conjugate gradient algorithm was adopted to optimize 3000 steps. The model was then optimized for energy minimization. The *NVT* ensemble (an ensemble of particles with a constant number of particles N, a constant volume V, and a constant temperature T) was used to balance 200 ps, and then the *NPT* (a constant pressure P) ensemble was used to balance 300 ps. The simulated temperature was 300 K, the MD simulation step was 1 fs, and the pressure was 1 atm (1 atm = 1.01325×10^5 Pa); the Andersen temperature control mode and the Berendsen pressure control mode were used.

2.1.3. Build epoxy resin cross-linking model

The crosslinking reaction process of DGEBA molecules and curing agent molecules are simulated in the subsubsection. The main reaction equation of DGEBA molecules with the amine curing agent is shown in Fig. 2(b). The principle of simulating the crosslinking reaction is to first select the carbon atoms in the DGEBA molecule that can undergo the crosslinking reaction, and then search for the nitrogen atoms on the curing agent molecular around a certain cut-off range. A chemical bond forms between the carbon atom and the nitrogen atom. In the process of forming carbon–nitrogen bond, the breaking of carbon–oxygen bond and the forming of carbon–nitrogen bond correspond to the opening of the ring of epoxy molecule and the crosslinking between epoxy molecule and curing agent molecule, respectively. The criterion for whether a crosslinking reaction can occur is the cut-off distance. First, 3.5 Å was set to be the cut-off distance, and all nitrogen atoms within 3.5 Å that can crosslink with carbon atoms were identified. As the degree of crosslinking increases, the formation of new chemical bonds becomes increasingly difficult. To accelerate the crosslinking reaction to the preset crosslinking degree, the cut-off distance was gradually increased to 8 Å in steps of 0.5 Å. Ideally, the crosslinking degree within the cut-off distance is 100%, but this is difficult to achieve in practice, so the crosslinking degree was set to be 90% and the reaction temperature was set to be 400 K. The process of simulating the crosslinking reaction was completed in the Perl language.

To make the model structure stable and closer to the real material, the crosslinked model was relaxed and quenched to eliminate the local internal stress of the model and make the density of the system close to the true value. The simulation for the case of running 100 ps at 500 K was conducted with the *NVT* ensemble, and then the *NPT* ensemble (an ensemble of particles with a constant number of particles N, a constant pressure P, and a constant temperature T) was used to simulate the case of running 500 ps at 500 K until the density and energy fluctuated are both in a very small range. The *NVT* and *NPT* ensembles were then used to cool the system from 500 K to 300 K at a cooling rate of 25 K per 400 ps (that is, every time the temperature drops by 25 K, the *NVT* ensemble is used to simulate the case of running 100 ps, and then the *NPT* ensemble is adopted to simulate the case of running 300 ps). Finally, the *NPT* ensemble was used to run 500 ps at 300 K to obtain the final model.

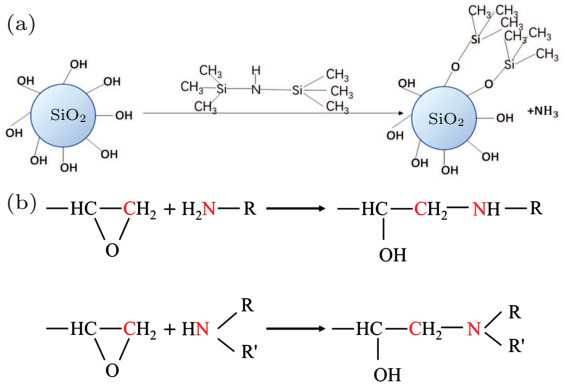


Fig. 2. (a) Reaction equation for surface grafting treatment of SiO_2 nanoparticles with HMDS. (b) Main reaction equation of DGEBA molecule and amine curing agent.

2.2. Simulation principle of thermal performance

In this study, the changes in the thermal properties of materials in terms of the glass transition temperature (T_g), coefficient of thermal expansion (CTE), and thermal conductivity, are mainly considered. The density and volume of EP change with temperature. When the temperature is lower than the T_g of EP, the EP is in a glassy state, and when the temperature is higher than the T_g of EP, the EP is in a rubbery state. The value of T_g can be obtained from the curve of specific volume (reciprocal of density) *versus* temperature. The intersection of the fitting line of temperature with the fitting line of specific volume refers to the T_g of EP when the temperature is higher and lower than T_g.[25–27]

The CTE is used to analyze the thermal expansion and contraction of a material as the temperature changes. The formula for calculating CTE is[26,27]

$$\mathrm{CTE} = \frac{1}{V_0}\left(\frac{\partial V}{\partial T}\right)_P, \tag{1}$$

where V_0 is the initial volume of the system and V is the volume of the system when the temperature is T. The CTE is related to the slope of the fitted line of specific volume versus temperature when the temperature is higher or lower than T_g. When calculating CTE, the value of V_0 when the material temperature is lower or higher than T_g is taken as the volume when the temperature is 300 K or 425 K, respectively.

The nonequilibrium molecular dynamics (NEMD) method was used to calculate the thermal conductivity of

the material. The NEMD method constructed a stable temperature gradient under a fixed heat flux, and then the thermal conductivity of the material was obtained by using Fourier's law.[28–30] In this study, the unit cell was divided into 20 parts in one direction, and the temperature of the material was taken as the average temperature of the model. The two edge layers were high-temperature layers and the middle two layers were low-temperature layers. The exchange of energy was achieved by exchanging the hottest particles in the cold layer with the coldest particles in the hot layer.

2.3. Principles of mechanical performance simulation

Mechanical properties are important indicators in the production and use of EP. This study simulated the changes in the bulk modulus, shear modulus, and Young's modulus of different materials at different temperatures. The static constant strain method was used to calculate the mechanical properties of the system, and a small strain was applied to the equilibrium EP system. Through the response of the system to strain, a simplified stiffness matrix C_{ij} could be obtained for isotropic amorphous materials as follows:[31,32]

$$C_{ij} = \begin{pmatrix} \lambda+2\mu & \lambda & \lambda & 0 & 0 & 0 \\ \lambda & \lambda+2\mu & \lambda & 0 & 0 & 0 \\ \lambda & \lambda & \lambda+2\mu & 0 & 0 & 0 \\ 0 & 0 & 0 & \mu & 0 & 0 \\ 0 & 0 & 0 & 0 & \mu & 0 \\ 0 & 0 & 0 & 0 & 0 & \mu \end{pmatrix}, \quad (2)$$

where λ and μ are the Lamé constants. The values of these constants can be obtained from the stiffness matrix as follows:

$$\lambda = \frac{1}{3}(C_{11}+C_{22}+C_{33}) - \frac{2}{3}(C_{44}+C_{55}+C_{66}), \quad (3)$$

$$\mu = \frac{1}{3}(C_{44}+C_{55}+C_{66}). \quad (4)$$

According to the values of λ and μ, the Young's modulus E, shear modulus G, and bulk modulus B can be obtained as follows:

$$E = \mu \cdot \frac{3\lambda+2\mu}{\lambda+\mu}, \quad (5)$$

$$G = \mu, \quad (6)$$

$$B = \lambda + \frac{2}{3}\mu. \quad (7)$$

By analyzing the changes in mean square displacement (MSD) with simulation time at different temperatures, the molecular chain-segment motion of the system could be determined. The greater the slope of the curve, the stronger the mobility of the molecular segment of the material is, which is a key factor affecting the mechanical properties of EP. The MSD is defined as[33,34]

$$\beta = \frac{1}{3N}\sum_{j=0}^{N-1}\left\langle \left|\boldsymbol{R}_j(t) - \boldsymbol{R}_j(0)\right|^2 \right\rangle, \quad (8)$$

where β is the MSD of the system, N is the total number of atoms in the system, and $\boldsymbol{R}_j(t)$ and $\boldsymbol{R}_j(0)$ are the displacement vector of any atom j in the system at time t and at the initial time, respectively. The angle brackets denote averaging over all chosen time origins.

The movement of molecular chains under the thermal field depends on the size of the free space. The polymer free volume ratio is given by

$$\alpha = \frac{V_f}{V_0+V_f}, \quad (9)$$

where V_0 is the volume occupied by the molecules that constitute the substance and V_f is the volume that accommodates the free movement of molecular segments in the system.

3. Results and discussion

3.1. Thermal properties

The simulation results for the thermal performance of different models are shown in Fig. 3. Figure 3(a) shows the T_g values of the different models. Although doping with different types of SiO_2 nanoparticles gives a slight increase in T_g, it is not much different from the undoped case. The T_g values of all models lie in a range of 402 K–410 K.

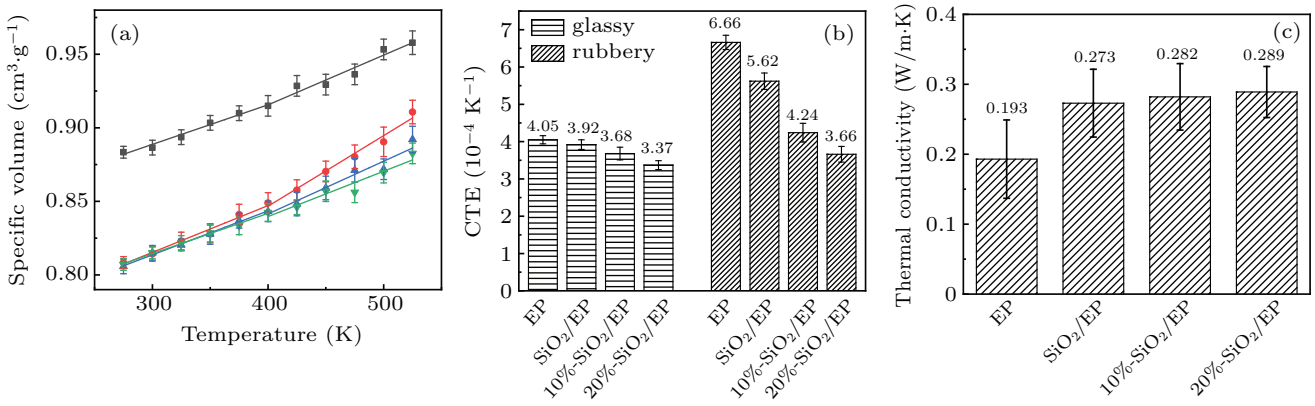


Fig. 3. Thermal performance simulation results, showing (a) change in specific volume with temperature, with vertical line denoting glass transition temperature, (b) thermal expansion coefficients of different materials in glassy state and rubbery state, and (c) thermal conductivities of different materials at 300 K.

Figure 3(b) shows the CTE values of different models in the glassy state and the rubbery state. The doping of SiO_2 nanoparticles reduces the CTE of the system. If SiO_2 is surface grafted, this suppression effect is more significant, and a higher grafting rate produces a lower CTE value. When the surface grafting ratio is 20%, the CET value in the glassy state and rubbery state are only 83.2% and 54.9% of those for undoped EP, respectively. This shows that the thermal expansion and contraction of EP are both suppressed. This may be related to the small CTE of SiO_2 nanoparticles and the strong interaction between SiO_2 and EP molecules. The effect of a higher grafting rate producing a lower CTE value may be due to the increased affinity of SiO_2 molecules and EP molecules after surface grafting, which makes the interaction between SiO_2 and EP molecules more intense. The specific analysis is described in more detail in the EP molecular density distribution map around the SiO_2 nanoparticles in next subsection.

Figure 3(c) shows the changes in thermal conductivity of different models at room temperature. After doping SiO_2 nanoparticles, the thermal conductivity is slightly higher than that of the undoped system. According to the Maxwell–Eucken model, the thermal conductivity of a composite material is given by the following equation:[23]

$$\lambda = \frac{\lambda_p\left[2\lambda_p + \lambda_f + 2V_f\left(\lambda_f - \lambda_p\right)\right]}{2\lambda_p + \lambda_f - V_f\left(\lambda_f - \lambda_p\right)}, \tag{10}$$

where λ, λ_p, and λ_f are the thermal conductivity of the composite, polymer, and filler, respectively, and V_f is the volume fraction of the filler. The thermal conductivity of EP is generally 0.2 W/(m·K), and that of SiO_2 is 1.4 W/(m·K). According to the above formula, the thermal conductivity of SiO_2/EP is 0.235 W/(m·K). The thermal conductivity of EP is close to the simulation result, but the thermal conductivity of doped SiO_2 is slightly lower than the simulation result. This is mainly because the model ignores the influence of the formation of thermally conductive chains, so the thermal conductivity of the compound calculated by the model is slightly lower than that of the actual material.[25] After the surface grafting treatment of SiO_2 nanoparticles, the thermal conductivity of the system further increases, but not significantly. The reason for this can be analyzed by using the Agari model[35,36]

$$\lg\lambda = V_f C_2 \lg\lambda_f + (1 - V_f)\lg(\lambda_p C_1), \tag{11}$$

where C_1 is a free factor for forming a thermally conductive chain and C_2 is a coefficient for the degree of difficulty of the filler forming a thermally conductive chain. This shows that after the surface grafting treatment of SiO_2 nanoparticles, the thermally conductive chains can form more easily, thereby improving the thermal conductivity of the system.

3.2. Mechanical properties

The MSD values of different models at different temperatures are shown in Fig. 4.

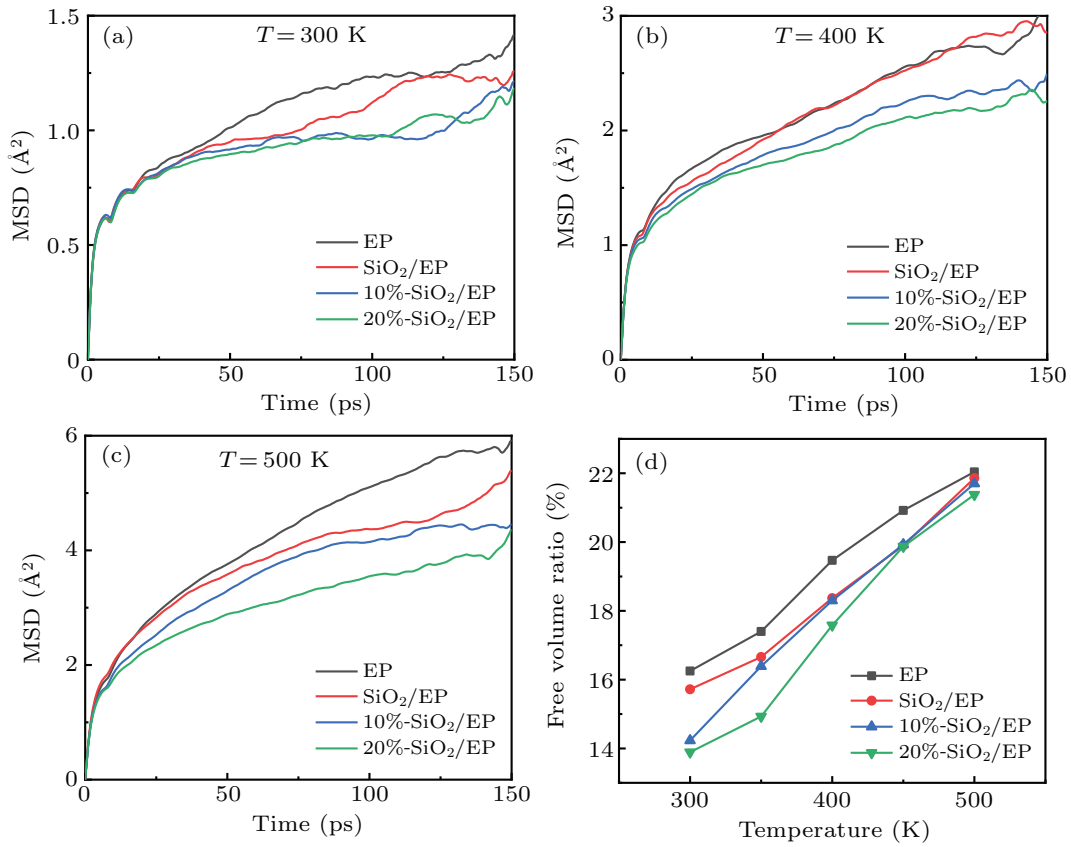


Fig. 4. Curves of MSD *versus* time at (a) 300 K, (b), 400 K, and (c) 500 K; (d) curves of free volume ratio *versus* temperature.

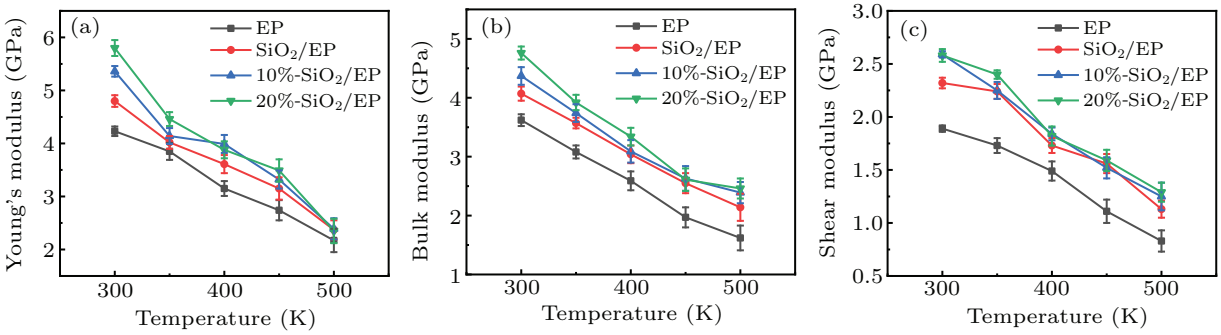


Fig. 5. Simulation results of mechanical properties: temperature-dependent (a) Young's modulus, (b) bulk modulus, and (c) shear modulus.

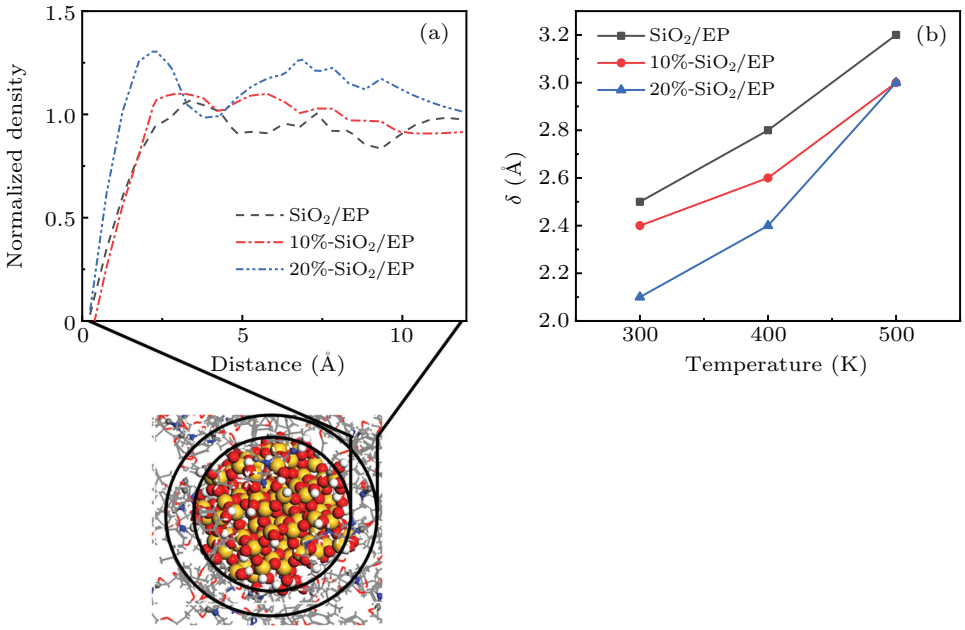


Fig. 6. Behaviors of EP molecules in the interface area, showing (a) normalized EP molecular density in the interface area, and (b) temperature-dependent thickness of the van der Waals excluded region.

At different temperatures, the MSD value generally conforms to the following order: EP>SiO_2/EP>10%-SiO_2/EP>20%-SiO_2/EP. This shows that the doping of SiO_2 nanoparticles effectively inhibits the movement of molecular chains in the system, especially the surface-grafted SiO_2 nanoparticles. Figure 4(d) shows the free volume ratios at different temperatures. From this figure, it is apparent that the free volume ratio exhibits similar properties. This is because the degree of molecular chain motion mainly depends on the proportion of free volume. At room temperature, the free volume ratio after doping with 20% surface-grafted SiO_2 nanoparticles is only 85.48% of that of EP. As the temperature increases, the MSD value and the free volume ratio gradually increase, indicating that a rising temperature enhances the degree of molecular chain movement.

Figure 5 shows the simulation results for the Young's modulus, bulk modulus, and shear modulus. After doping with SiO_2 nanoparticles, especially surface-grafted SiO_2 nanoparticles, these values are improved, indicating that the mechanical properties have been improved. The reason for this is that in addition to the inhibition of the molecular segment movement mentioned above, there is stronger interaction between SiO_2 and EP molecules.

Figure 6(a) shows the density distribution of EP molecules around SiO_2 nanoparticles. After doping with SiO_2 nanoparticles, an interface region forms around the surface. In this interface area, the molecular density of EP is very low when it is less than 2.5 Å from the surface of the SiO_2 nanoparticles. This area is also called the van der Waals excluded region. The thickness of this area is defined as follows:[37]

$$(r_{\mathrm{NP}}+\delta)^3 - r_{\mathrm{NP}}^3 = \int_0^{\infty} r^2(1-\rho_{\mathrm{r}}/\rho_0)\,\mathrm{d}r, \qquad (12)$$

where δ is the region thickness, r_{NP} is the radius of the nanoparticle, ρ_{r} is the radial density from the surface of the nanoparticle to a given distance r, and ρ_0 is the polymer bulk density of the system. At 300 K, after doping with SiO_2 nanoparticles, the thickness of the van der Waals excluded region is 2.5 Å, whereas after doping with 10% and 20% surface-grafted SiO_2 nanoparticles, the thickness values of the van der Waals repelling zone become 2.4 Å and 2.1 Å, respectively. This shows that chemical modification of the SiO_2

nanoparticles weakens the molecular repulsion force between SiO_2 nanoparticles and EP, which is consistent with the understanding that the compatibility between SiO_2 nanoparticles and polymers can be improved after grafting treatment. Figure 6(b) shows the variations of δ with temperature at different temperatures. It can be seen that at any temperature, δ for the grafted SiO_2 nanoparticles is lower than that in the nongrafted case, and a higher grafting rate produces a lower value of δ, which means that there is a higher density of EP molecules in the interface region. A higher molecular density corresponds to the better elastic properties, that is, better mechanical properties. This is also why the mechanical properties of the materials runs in the order 20%-SiO_2/EP>10%-SiO_2/EP>SiO_2/EP. This is true at different temperatures, indicating that this material modification method has good thermal stability.

4. Conclusions

This study presents the results of MD simulations in which the SiO_2 nanoparticles and SiO_2 nanoparticles grafted with HMDS at 10% and 20% surface grafting rates are doped into epoxy resin. The thermal and mechanical properties of these nanodielectrics and the microscopic mechanisms were studied in depth. The main conclusions are as follows.

(i) After doping with SiO_2 nanoparticles, the glass transition temperature does not change significantly. However, the thermal expansion and contraction of the system and the thermal conductivity are improved, especially by the surface grafting treatment of SiO_2 nanoparticles. The main reason may be that after the surface grafting treatment, the thermal chains can form more easily.

(ii) After doping with SiO_2 nanoparticles, the mechanical properties of the system are significantly improved. Of the systems considered in this study, the improvement in mechanical properties can be ordered as follows: 20%-SiO_2/EP>10%-SiO_2/EP>SiO_2/EP>EP. We think, this is mainly related to two factors. First, the doping of SiO_2 nanoparticles inhibits the degree of movement of the molecular chains in the system, so SiO_2/EP>EP. Second, after the surface grafting treatment, the molecular repulsion between SiO_2 and EP is weakened, and the van der Waals excluded region becomes thinner, that is, the compatibility between SiO_2 nanoparticles and polymer is improved by the grafting treatment. Thus, the mechanical properties are further improved, leading to the ordering 20%-SiO_2/EP>10%-SiO_2/EP>SiO_2/EP.

Based on the analysis in this article, we believe that the surface grafting treatment of SiO_2 nanoparticles with HMDS and then doping into epoxy resin can effectively improve the thermal and mechanical properties of the system, and has strong potential practical applications in future.

References

[1] Wang T, Zhang G, Li D, Hou Y and Zhang B 2020 *IEEE Trans. Dielectr. Electr. Insul.* **27** 939
[2] Wang T, Zhang B, Li D, Hou Y and Zhang G 2020 *Nanotechnol.* **31** 324001
[3] Du B, Han C, Li J and Li Z 2020 *IEEE Trans. Dielectr. Electr. Insul.* **27** 418
[4] Wang Y, Wu J, Yin Y and Han T 2020 *IEEE Trans. Dielectr. Electr. Insul.* **27** 377
[5] Yao T, Chen K, Shao T, Zhang C, Zhang C and Yang Y 2020 *IEEE Trans. Dielectr. Electr. Insul.* **27** 528
[6] Wang T, Li D, Hou Y and Zhang G 2020 *High Volt. Eng.* **46** 4129 (in Chinese)
[7] Chu P, Zhang H, Zhao J, Gao F, Guo Y, Dang B and Zhang Z 2017 *Compos. Pt. A-Appl. Sci. Manuf.* **99** 139
[8] Yang J, Zhu Z, Huang D and Cao Q 2020 *Chin. Phys. B* **29** 023104
[9] An M, Su M, Deng Q, Song H, Wang C and Shang Y 2020 *Chin. Phys. B* **29** 046201
[10] Xu W, Wu Y, Zhu Y and Liang X 2020 *Chin. Phys. B* **29** 046601
[11] Shen X, Wang Z, Wu Y, Liu X, He Y and Kim J 2016 *Nano Lett.* **16** 3585
[12] Wang Z, Lv Q, Chen S, Li C, Sun S and Hu S 2016 *ACS Appl. Mater. Interfaces* **8** 7499
[13] Fasanelia N and Sundararaghavan V 2016 *JOM* **68** 1
[14] Gou J, Minaie B, Wang B, Liang Z and Zhang C 2004 *Comput. Mater. Sci.* **31** 225
[15] Jung H, Choi H, Kim S, Lee H, Kim Y and Yu J 2017 *Compos. Pt. A-Appl. Sci. Manuf.* **103** 17
[16] Diao Z, Zhao Y, Chen B, Duan C and Song S 2013 *J. Anal. Appl. Pyrolysis* **104** 618
[17] Han Z, Zou L, Xin Z, Zhao T and Zhang L 2018 *Trans. China Electr. Society* **33** 4692 (in Chinese)
[18] Zhang Y, Li J, Wang J, Yang X, Shao W, Xiao S and Wang B 2014 *RSC Adv.* **4** 17083
[19] Lu X, Wang X, Li Q, Huang X, Han S and Wang G 2015 *Polym. Degrad. Stabil.* **114** 72
[20] Liu X, Li X, Liu J, Wang Z, Kong B, Gong X, Yang X, Lin W and Li G 2014 *Polym. Degrad. Stabil.* **104** 62
[21] Rahnamoun A and Duin A 2014 *J. Phys. Chem. A* **118** 2780
[22] Li Q, Huang X, Liu T, Yan J, Wang Z, Zhang Y and Lu X 2016 *Trans. China Electr. Society* **31** 1 (in Chinese)
[23] Wang T, Zhang G, Li D and Hou Y 2020 *J. Appl. Phys.* **128** 025101
[24] Shen L, Zou L, Ding M, Zhao T, Zhang L and Li Q 2020 *Appl. Surf. Sci.* **505** 144197
[25] Bandyopadhyay A, Valavala P, Clancy T, Wise K and Odegard G 2011 *Polymer* **52** 2445
[26] Li C and Strachan A 2015 *J. Polym. Sci. Pt. B-Polym. Phys.* **53** 103
[27] Masoumi S, Arab B and Valipour H 2015 *Polymer* **70** 351
[28] Jund P and Jullien R 1999 *Phys. Rev. B* **59** 13707
[29] Plathe F 1997 *J. Chem. Phys.* **106** 6082
[30] Ju S, Haung T, Liao C and Chang J 2013 *Polymer* **54** 4702
[31] Zhang W, Qing Y, Zhong W, Sui G and Yang X 2017 *React. Funct. Polym.* **111** 60
[32] Shokuhfar A and Arab B 2013 *J. Mol. Model.* **19** 3719
[33] Zhang W, Li H, Gao L, Zhang Q, Zhong W, Sui G and Yang X 2018 *Polym. Compos.* **39** E945
[34] Yang Q, Yang X, Li X, Lei S and Sui G 2013 *RSC Adv.* **3** 7452
[35] Agari Y, Ueda A and Nagai S 1993 *J. Appl. Polym. Sci.* **49** 1625
[36] Agari Y, Ueda A and Nagai S 1991 *J. Appl. Polym. Sci.* **43** 1117
[37] Voyiatzis E, Rahimi M, Muller-Plathe F and Bohm M 2014 *Macromolecules* **47** 7878